ORGANIC LETTERS

2008
Vol. 10, No. 14
2943−2946

Designing Functionalized Porphyrins Capable of Pseudo-2D Self-Assembly on Surfaces

Sheshanath V. Bhosale,[†] Mark A. Bissett,[‡] Craig Forsyth,[†] Steven J. Langford,*[,†] Suzanne M. Neville,[†] Joseph G. Shapter,*[,‡] Laura Weeks,[‡] and Clint P. Woodward[†]

School of Chemistry, Monash University, Clayton, Victoria 3800, Australia, School of Chemistry, Physics and Earth Sciences, Flinders University of South Australia, Bedford Park, South Australia 5042, Australia

steven.langford@sci.monash.edu.au; joe.shapter@flinders.edu.au

Received April 17, 2008

ABSTRACT

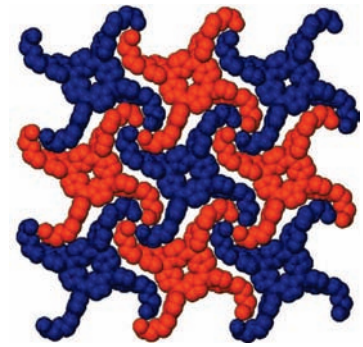

A crystallography-instructed strategy to highly ordered layering of porphyrins with different topologies on HOPG is developed based on *meso*-tetraarylporphyrins bearing 2-ethoxyethanol side chains as "sticky ends". These sticky ends are capable of displaying directive hydrogen bonding motifs with the inherent D_{4h} symmetry of the porphyrins. Solvent effects are shown to have an important role in fabricating the adsorption. Metalation and subsequent axial ligation was a key controlling factor in the topology of the layer, leading to pseudo-2D structures on HOPG.

Molecular devices and sensors fabricated on surfaces, especially redox-active ones, have the potential to provide a reliable transfer of molecular function to the macroscopic world. However, the controlled deposition and organization of organic/supramolecular components on solid surfaces still represents a key challenge. One attractive approach exploits molecular recognition leading to highly and long-range ordered, functional structures.[1] Of the potential classes of compounds for use in molecular devices and sensors, porphyrins are often employed because of their favorable chemical, electronic, and photophysical properties.[2] Controlling the arrangement of metalloporphyrins into well-defined and ordered 2D arrays is aided by the inherent D_{4h} symmetry of the parent macrocycle. The desired control may be executed by utilizing "intelligent" porphyrins which possess preprogrammed functionality to aid molecular alignment in either a *pseudo* 1D or 2D and 3D arrays, as demonstrated in both the solid state[3] and on solid surfaces.[4] The ability to

[†] Monash University.
[‡] Flinders University of South Australia.

(1) (a) De Feyter, S.; De Schryver, F. C. *Chem. Soc. Rev.* **2003**, *32*, 139–150. (b) De Feyter, S.; De Schryver, F. C. *J. Phys. Chem. B* **2005**, *109*, 4290–4302. (c) Elemans, J. A. A. W.; Van Hameren, R.; Nolte, R. J. M.; Rowan, A. E. *Adv. Mater.* **2006**, *18*, 1251–1266. (d) Wang, T.; Bhosale, Sh.; Bhosale, Si.; Li, G.; Fuhrhop, J.-H. *Acc. Chem. Res.* **2006**, *39*, 498–508.

(2) (a) Burrell, A. K.; Wasielewski, M. R. *J. Porphyrins Phthalocyanines* **2000**, *4*, 401–406. (b) Purrello, R.; Gurrieri, S.; Lauceri, R. *Coord. Chem. Rev.* **1999**, *192*, 683–706. (c) Rakow, N. A.; Suslick, K. S. *Nature* **2000**, *406*, 710–713. (d) Wu, D. G.; Cahen, D.; Graf, P.; Naaman, R.; Nitzan, A.; Shvarts, D. *Chem. Eur. J.* **2001**, *7*, 1743–1749. (e) Kosal, M. E.; Suslick, K. S. *J. Solid State Chem.* **2000**, *152*, 87–98. (f) Kosal, M. E.; Chou, J.-H.; Wilson, S. R.; Suslick, K. S. *Nat. Mater.* **2002**, *1*, 118–121.

10.1021/ol800895q CCC: $40.75
Published on Web 06/17/2008

self-assemble becomes exceedingly important under mild conditions of physisorption and ambient temperature and pressure where molecular motion of the absorbed species can play a significant role. Moreover, the chance for axial ligation offers the opportunity for layering of other molecular species into more elaborate systems. Utilization of a real time, noninvasive imaging technique such as STM[1,5] allows direct assessment of surface modifications after each sequential component addition cycle, without disturbing the molecular positioning effected by the noncovalent interactions between components. Conducting materials of high atomic smoothness, such as atomically flat gold[6] and highly oriented pyrolytic graphite (HOPG),[7] provide an appropriate base on which to build and image molecular constructs. In this paper we report on the development of an ordering strategy using porphyrins with *meso*-(4-phenyl(2-(2-ethoxy)ethanol)) side chains (so-called TEEP) on HOPG. X-ray crystallography and scanning probe microscopy (SPM) techniques have been used to evaluate the design strategy and characterize the materials formed in the solid state.

The choice of motif was predicated in a report which noted that the pendant 2-ethoxyethanol arms self-associate by an unusual hydrogen bonding motif to form a tape within a C_{2v}

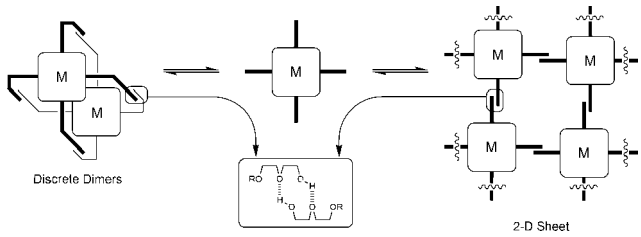

Figure 1. Utilizing the potential of 2-(2-ethoxy)ethanol groups on the porphyrin periphery to hydrogen bond may lead to a ordered supramolecular constructs. One possible hydrogen bonding motif using 2-ethoxyethanol groups is highlighted.

symmetrical system.[8] In a porphyrin exhibiting D_{4h} symmetry, such functionality could potentially self-assemble cooperatively,

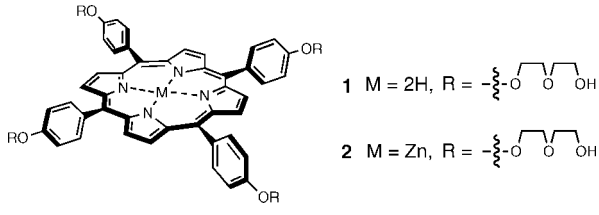

Figure 2. Porphyrins used in this study. Porphyrin derivatives bearing 2-(2-ethoxy)ethanol groups have been given the acronym TEEP (TetraEthoxyEthanolPorphyrin).

forming two distinct intermolecular hydrogen bonds per ethoxyethanol set leading to discrete capsular assemblies or 2D supramolecular arrays (Figure 1). Compound **1**[9] (Figure 2) is surprisingly insoluble in the usual aprotic solvents used for dissolving tetraphenylporphyrins (e.g., $CHCl_3$, CH_2Cl_2, toluene). This insolubility can be attributed to intermolecular hydrogen bonding interactions, which are desirable but uncontrolled to this point. The problem is alleviated by the addition of a small amount of a solvent capable of interfering with hydrogen bonding (e.g., methanol or DMF or pyridine (py)). Differential scanning calorimetry (DSC) was used to probe the changes in **1** as a function of temperature. A reproducible DSC trace was obtained, showing three broad second order endotherms at onset temperatures of approximately 40, 120, and 210 °C (see Supporting Information). Compound **1** melts at approximately 260 °C.

Zinc metalation of **1** was achieved using the acetate method[10] ($Zn(OAc)_2$/DCM/MeOH) producing **2** in 89% yield. Solubility of porphyrin **2** was also only possible in a mixed solvent system in which a solvent capable of competing with the ethoxyethanol hydrogen bonding was employed. Manipulating the solubility of **1** and **2** by protic means may be advantageous during surface deposition, as it provides an external control for triggering the layering of the porphyrin from solution when coated over the surface. Since a relationship between the packing of molecules in the solid state and the patterning observed when deposited onto a surface exists,[11] solid-state structures can be used as a means of predicting how the same molecule might organize on a two-dimensional surface.

Single crystals of **1** suitable for X-ray structure determination were grown by the slow diffusion of acetone into a DMF solution of the porphyrin (Figure 3).[12] Porphyrin **1** adopts a saddle (*sad*) conformation with deviation in atomic displace-

(3) (a) Kobayashi, K.; Koyanagi, M.; Endo, K.; Masuda, H.; Aoyama, Y. *Chem. Eur. J.* **1998**, *4*, 417–424. (b) Diskin-Posner, Y.; Patra, G. K.; Goldberg, I. *Eur. J. Inorg. Chem.* **2001**, *251*, 5–2523. (c) Vinodu, M.; Goldberg, I. *CrystEngComm* **2004**, *6*, 215–220. (d) Vinodu, M.; Goldberg, I. *CrystEngComm* **2005**, *7*, 133–138.

(4) (a) Thomas, P. J.; Berovic, N.; Laitenberger, P.; Palmer, R. E.; Bampos, N.; Sanders, J. K. M. *Chem. Phys. Lett.* **1998**, *294*, 229–232. (b) Yokoyama, T.; Yokoyama, S.; Kamikado, T.; Okuno, Y.; Mashiko, S. *Nature* **2001**, *413*, 619–621. (c) Yokoyama, T.; Kamikado, T.; Yokoyama, S.; Mashiko, S. J. *J. Chem. Phys.* **2004**, *121*, 11993–11997. (d) Drain, C. M.; Batteas, J. D.; Flynn, G. W.; Milic, T.; Chi, N.; Yablon, D. G.; Sommers, H. *Proc. Natl. Acad. Sci. U.S.A.* **2002**, *99*, 6498–6502. (e) Bonifazi, D.; Spillmann, H.; Kiebele, A.; de Wild, M.; Seiler, P.; Cheng, F.; Güntherodt, J.; Jung, T.; Diederich, F. *Angew. Chem., Int. Ed* **2004**, *43*, 4759–4763. (f) Suzuki, H.; Yamada, T.; Kamikado, T.; Okuno, Y.; Mashiko, S. *J. Phys. Chem. B* **2005**, *109*, 13296–13300. (g) Bonifazi, D.; Kiebele, A.; Stöhr, M.; Cheng, F.; Jung, T.; Diederich, F.; Spillmann, H. *Adv. Funct. Mater.* **2007**, *17*, 1051–1062. (h) Hai, N. T. M.; Gasparovic, B.; Wandelt, K.; Broekmann, P. *Surf. Sci.* **2007**, *601*, 2597–2602. (i) Wintjes, N.; Bonifazi, D.; Cheng, F.; Kiebele, A.; Stöhr, T, M.; Jung, T.; Spillmann, H.; Diederich, F. *Angew. Chem., Int. Ed.* **2007**, *46*, 4089–4092.

(5) (a) Palmer, R. E.; Guo, Q. *Phys. Chem. Chem. Phys.* **2002**, *4*, 4275–4284. (b) Louder, D. R.; Parkinson, B. A. *Anal. Chem.* **1994**, *66*, 84–105.

(6) Lusic, D.; Shapter, J. G.; Gooding, J. J. *Aust. J. Chem.* **2001**, *54*, 643–648.

(7) Bampos, N.; Woodburn, C. N.; Welland, M. E.; Sanders, J. K. M. *Angew. Chem., Int. Ed.* **1999**, *38*, 2780–2783.

(8) Cubberley, M. S.; Iverson, B. L. *J. Am. Chem. Soc.* **2001**, *123*, 7560–7563.

(9) Langford, S. J.; Woodward, C. P. *Polyhedron* **2007**, *26*, 338–343.

(10) Buchler, J. W. In *Porphyrins and Metalloporphyrins*; Smith, K. M., Ed. Elsevier: New York, 1976; pp 179−181.

(11) (a) Hill, J. P.; Wakayama, Y.; Schmitt, W.; Tsuruoka, T.; Nakanishi, T.; Zandler, M. L.; McCarty, A. L.; D'Souza, F.; Milgrom, L. R.; Ariga, K. *Chem. Commun.* **2006**, 2320–2322. (b) Hill, J. P.; Wakayama, Y.; Akada, M.; Ariga, K. *J. Phys. Chem. C* **2007**, *111*, 16174–16180. (c) Yoshimoto, S.; Yokoo, N.; Fukuda, T.; Kobayashi, N.; Itaya, K. *Chem. Commun.* **2006**, 500–502.

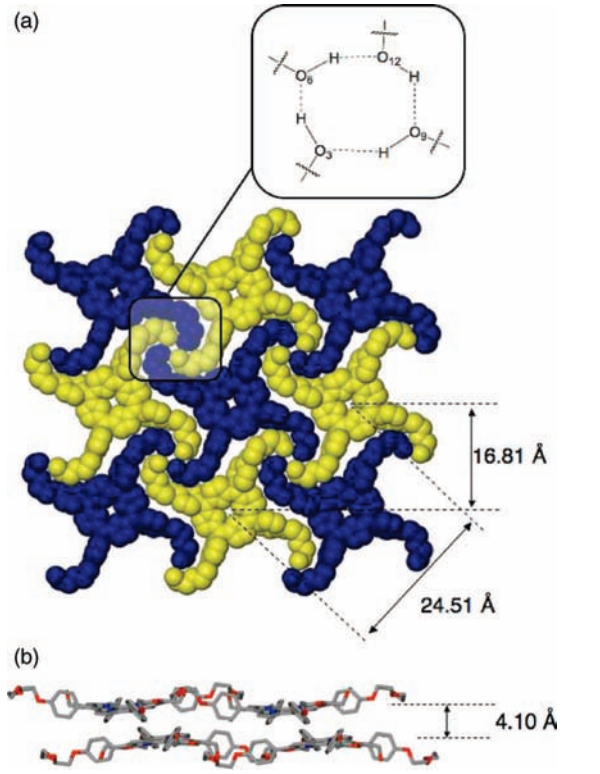

Figure 3. (a) Entwined arrangement of **1** in the solid state. Insert highlights the eight-membered cyclic H-bonding motif. Center-to-center distances between adjacent and diagonally positioned porphyrins within a 2D sheet. (b) Interlayer distance separating the porphyrin sheets of 4.10 Å. Noncritical hydrogen atoms have been omitted for clarity in all views.

ments from the mean macrocycle plane of up to 0.37 Å.[13] Despite their inherent flexibility, the 2-ethoxyethanol chains show little disorder, with the internal OCH_2CH_2O groups and the terminal OCH_2CH_2OH group all orienting in a staggered *gauche* arrangement. Instead of the expected hydrogen bonding pattern, four ethoxyethanol side arms of independent porphyrin molecules become entwined, driven by the terminal hydroxyl groups that hydrogen bond (O···O = 2.751−2.830 Å) effectively but in an alternative eight-membered macrocycle of *pseudo*-square geometry (Figure 3a). Center-to-center separation distances of the porphyrins contained within the sheets are found to be 16.81 Å for adjacent porphyrins and 24.51 Å for porphyrins located along a diagonal direction (Figure 3a). A promising feature of this crystal structure is that **1** orders into two-dimensional sheets, driven by hydrogen bonding. Each porphyrin sheet is separated by an average interplane distance of 4.10 Å (Figure 3b).

A complication in this design strategy arises when axial ligation competes with hydrogen bonding as is the case of **2**, leading to the formation of a dimer in the solid state (Scheme 1).[9] The addition of pyridine (py) was made to act as a competing group capable of strong coordination (10^4 M^{-1}) to the zinc metal ion. The effect was to displace the weakly coordinated alcohol sidearm from the porphyrin's zinc center so as to utilize the polyether chains for two-dimensional hydrogen bonded assembly (Scheme 1). In this way, the complex **2**·py could be viewed as a prototype to layered ensembles.

Scheme 1. Manipulation of Dimerization of **2** Used as a Strategy for Preparing Pseudo-2D sheets

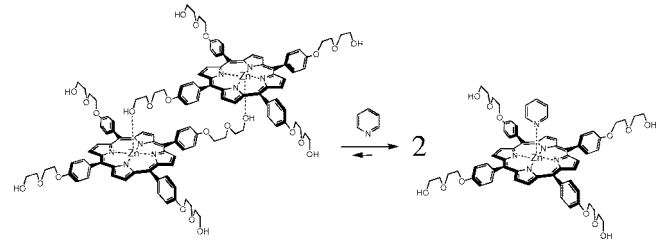

This adjustment proved to be an effective crystal growth strategy. Rectangular red plate crystals of **2**·py suitable for X-ray structure determination were obtained by slow diffusion of hexane into a THF/pyridine solution of **2**.[14] The crystal structure reveals the axial ligation of pyridine to the Zn(II) center (disordered over two positions) allowing the polyether arms to protrude away from the macrocyclic core (Figure 4). The pyridine complexation has a pronounced effect on the supramolecular packing arrangement of **2**, reverting the observed dimer[10] back to a monolayer sheeting arrangement. In this case however, the observed intermolecule stabilization motif displays a different arrangement to that previously seen for **1** (Figure 4). The axially coordinated pyridine ligands of one layer sit in the void cavities within the two-dimensional porphyrin sheet network with the remaining vacant space occupied by clathrate THF solvent. Two-dimensional sheets are separated by an average interplane distance of 4.2 Å.

The structural insights obtained from the solid-state analysis of **1** and **2**·py infer that this class of molecules possess a high propensity to form two-dimensional porphyrin

(12) Crystal data for **1**: $C_{60}H_{62}N_4O_{12}$, M = 1031.15, red plate, 0.31 × 0.28 × 0.15 mm^3, triclinic, space group P-1, a = 9.7441(8), b = 16.1523(11), c = 17.6166(14) Å, α = 80.484(4)°, β = 75.436(4)°, γ = 76.515(4)°, V = 2592.8(3) Å^3, Z = 2, D_c = 1.321 g/cm^3, F_{000} = 1092, T = 150(2)K, $2q_{max}$ = 63.6°, 78075 reflections collected, 17629 unique (R_{int} = 0.0299). Final GoF = 1.161, $R1$ = 0.0993, $wR2$ = 0.2273, R indices based on 14264 reflections with $I > 2s(I)$ (refinement on F^2), 685 parameters. Crystallographic data for **1** has been deposited with the Cambridge Crystallographic Data Centre as supplementary publication no. CCDC-664957. Copies of the data can be obtained free of charge on application to CCDC, 12 Union Road, Cambridge CB21EZ, U.K. Fax: (+44)1223-336-033. E-mail: deposit@ccdc.cam.ac.uk.

(13) Scheidt, W. R. In *The Porphyrin Handbook*, 1st ed.; Kadish, K. M., Smith, K. M., Guilard, R., Eds.; Academic Press: San Deigo, 2000; Vol. 3, pp 49−112.

(14) Crystal data for **2**·py (THF): $C_{69}H_{73}N_5O_{13}Zn$, M = 1245.69, red plate, 0.10 × 0.10 × 0.03 mm^3, triclinic, space group P-1, a = 9.1436(5), b = 13.1247(6), c = 16.1132(9) Å, α = 73.900(3)°, β = 89.751(3)°, γ = 71.603(2)°, V = 1755.55(16) Å^3, Z = 1, D_c = 1.178 g/cm^3, F_{000} = 656, T = 123(2)K, $2q_{max}$ = 40°, 14282 reflections collected, 3267 unique (R_{int} = 0.070), Final GoF = 1.201, $R1$ = 0.1634, $wR2$ = 0.3757, R indices based on 2972 reflections with $I > 2s(I)$ (refinement on F^2), 250 parameters, 92 restraints. Crystallographic data for **2**·py has been deposited as supplementary publication no. CCDC-664958.

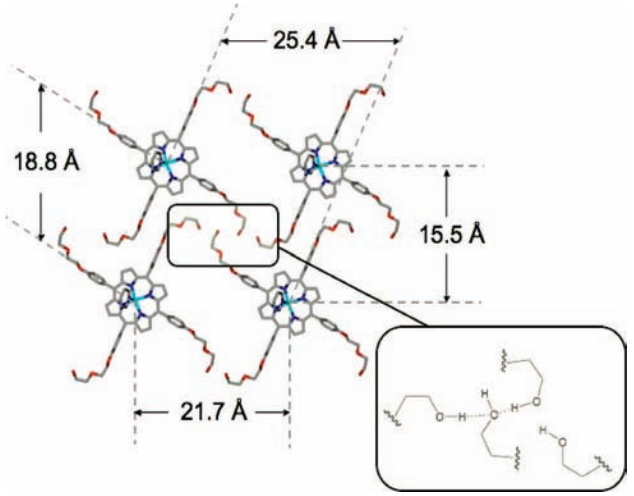

Figure 4. (a) X-ray crystal structure representation of **2**•py displaying the H-bonding motif (H atoms omitted for clarity). Center-to-center distances between adjacent and diagonally positioned porphyrins within a 2D sheet are also given.

sheets by hydrogen bonding provided metal ion−ethoxyethanol interactions can be minimized. The solution studies indicate that the hydrogen bonding and hence the molecular packing arrangements can be easily manipulated by alteration of the solvent system used to solvate the structural components. With this in mind, liquid-phase deposition of **1** (in $CHCl_3$/MeOH solvent) or **2** (in $CHCl_3$/pyridine solvent) from 1×10^{-6} M solutions on HOPG followed by evaporation allows for the formation of an ultrathin film on the surface. The associated spreading and evaporation of the solution leads to an ordered surface deposition, as evinced by the STM images of **1** and **2**•py (Figure 5) obtained under ambient conditions. These patterns differ strongly to that observed for HOPG under the same conditions. The ambient conditions used do not lead, as expected, to molecular resolution but rather a defined patterning effect.

STS curves of the HOPG treated with **1** and **2**•py confirm the presence of the porphyrin layers (Supporting Information). The two main peaks in both STS curves, one located at −1.75 V and the other at 0.55 V for **1** and 0.71 V for **2**•py, corresponding very well with literature values for free base and ZnTPP for this technique.[15] The molecular film prepared by **1** has intermolecular spacing of 1.2 nm commensurate with the close face-on-face tilt packing of the molecules along the surface (Figure 5d) in which the porphyrin−porphyrin interactions compete favorable against the porphyrin−HOPG interactions. For **2**•py adsorbed on HOPG, the intermolecular spacing of the porphyrins along the rows is on average 5.67 nm, the spacing between adjacent rows is 4.40 nm. This nonsymmetric pattern is expected on the basis of the planar adsorption of the porphyrin macrocycles and the intermolecular interactions observed in the

(15) (a) Nishino, T.; Ito, T.; Umezawa, Y. *Proc. Natl. Acad. Sci. U.S.A.* **2005**, *102*, 5659–5662. (b) Scudiero, L.; Barlow, D. E.; Mazur, U.; Hipps, K. W. *J. Am. Chem. Soc.* **2001**, *123*, 4073–4080.

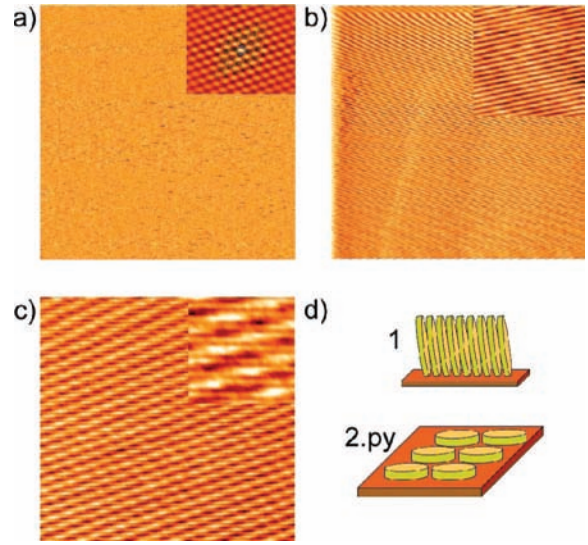

Figure 5. Room temperature and pressure STM images of (a) 100 nm × 100 nm image of HOPG; inset is a 2 nm × 2.5 nm scan of the substrate showing atomic resolution. The overlaid circles are the expected atomic spacings for HOPG. (b) 100 nm × 100 nm image of **1** deposited on HOPG, inset is a 15 nm × 15 nm zoom of the image. (c) 100 nm × 100 nm image of **2**•py deposited on HOPG, inset is a 15 nm × 15 nm zoom of the image. (d) Proposed edge generated by the deposition of **1** and **2**•py, respectively, on HOPG. Conditions: tungsten tip; scan rate = 3.05 Hz; Vt = 50 mV; It = 1.0 nA.

crystal structure. Importantly, the dramatically different patterning scales from **1** to **2**•py is attributable to the influence of the axial ligand.[16] The incorporation of the pyridine no longer allows efficient face-on packing, leading to the 2D layering observed for the porphytrin on HOPG.

In summary, a class of porphyrins, coined TEEP, that possess a pendant hydrogen bonding functionality, or sticky end, have been designed. The different crystal structure morphologies obtained of these TEEP molecules displayed varying styles of 2D sheeting, which is driven in each case by hydrogen bonding interactions, crystal packing forces, and in the case of **2**, metalloporphyrin coordination. Preliminary surface layering experiments of **1** and **2**•py have given a rudimentary proof-of-concept that TEEP molecules can form regular surface patterning that can be controlled by solvent effects and axial ligation. Studies pertaining to more exotic layering are underway.

Acknowledgment. This project is supported by Australian Research Council Discovery Project DP0556313 and DP0878220.

Supporting Information Available: Experimental procedures, sample preparation and characterization (STS, DSC, X-ray crystallography and STM imaging) for compounds **1** and **2**. This material is available free of charge via the Internet at http://pubs.acs.org.

OL800895Q

(16) The aberrant measurement of height at the layer-graphite interface supports the formation of two differently orientated films. In the case of **1** the lower tunnelling current is consistent with the face-to-face orientation of the layers. Higher tunnelling currents for **2**•py is consistent with its flat-packed arrangement.